

Enhanced sequential directional importance sampling for structural reliability analysis

Kai Cheng^{a*}, Iason Papaioannou^a and Daniel Straub^a

^a*Engineering Risk Analysis Group, Technical University of Munich, Theresienstr.
90, Munich, 80333, Germany*

Abstract

Sequential directional importance sampling (SDIS) [12] is an efficient adaptive simulation method for estimating failure probabilities. It expresses the failure probability as the product of a group of integrals that are easy to estimate, wherein the first one is estimated with Monte Carlo simulation (MCS), and all the subsequent ones are estimated with directional importance sampling. In this work, we propose an enhanced SDIS method for structural reliability analysis. We discuss the efficiency of MCS for estimating the first integral in standard SDIS and propose using Subset Simulation as an alternative method. Additionally, we propose a Kriging-based active learning algorithm tailored to identify multiple roots in certain important directions within a specified search interval. The performance of the enhanced SDIS is demonstrated through various complex benchmark problems. The results show that the enhanced SDIS is a versatile reliability analysis method that can efficiently and robustly solve challenging reliability problems.

Keywords: Reliability analysis; Directional importance Sampling; Monte Carlo; Markov Chain Monte Carlo;

1. Introduction

The fast evolution of computing power has enabled the development of various high-fidelity numerical models to simulate the performance of complex engineering systems in nearly all fields of engineering and science. Nevertheless, due to inevitable uncertainties involved in design, construction and operational conditions, the response of engineering systems remains uncertain. Reliability analysis is therefore an essential tool to assess the safety of

engineering structures. It is concerned with estimating the failure probability

$$P_f = \int_{g(\mathbf{x}) \leq 0} f_{\mathbf{X}}(\mathbf{x}) d\mathbf{x} = \int_{\mathbb{R}^n} I(g(\mathbf{x}) \leq 0) f_{\mathbf{X}}(\mathbf{x}) d\mathbf{x} = \mathbb{E}_{f_{\mathbf{X}}} [I(g(\mathbf{X}) \leq 0)], \quad (1)$$

where $\mathbf{X} = (X_1, \dots, X_n)^T$ is the n -dimensional continuous input random vector with joint probability density function (PDF) $f_{\mathbf{X}}(\mathbf{x})$, $g(\mathbf{x})$ is the limit state function (LSF), and $I(\cdot)$ is the indicator function, which gives 1 if failure occurs, i.e., if $g(\mathbf{x}) \leq 0$, and 0 otherwise. $\mathbb{E}_{f_{\mathbf{X}}}[\cdot]$ denotes the expectation operator with respect to the density $f_{\mathbf{X}}(\mathbf{x})$.

During the last few decades, various reliability analysis methods have been developed, and they can be categorized into four types: approximate analytical methods [23, 15], numerical integration methods [49, 46], surrogate-assisted methods [17, 10, 41, 33] and numerical simulation methods [2, 36, 20, 37]. The approximate analytical methods approximate the LSF by low-order Taylor expansions to estimate the failure probability. These include the first order reliability method (FORM) [26] and the second order reliability analysis method (SORM) [6, 29]. However, the accuracy of these method can be low for highly non-linear problems. With numerical integration methods, the first few moments of the LSF are computed by the point estimation method [49] or sparse grid integration method [24], and the model response PDF as well as the the failure probability are estimated based on these moments. These methods suffer from the ‘‘curse of dimensionality’’, i.e., the associated computational cost rises sharply with the input variable dimension. Surrogate-assisted methods first fit a surrogate model based on a set of training points to approximate the true LSF, and then perform reliability analysis efficiently using the cheap-to-evaluate surrogate model. Recently, various surrogate model-based active learning strategies have been developed for reliability analysis [17, 41, 33, 13, 44]. However, these methods only work for low-to-moderate dimensional problems. Numerical simulation methods, based on Monte Carlo simulation (MCS), are generally preferred for reliability analysis of complex engineering systems due to their robustness. In this category, various variance reduction methods have been developed, including: importance sampling (IS) [1, 3], sequential importance sampling (SIS) [36, 45], cross-entropy based adaptive IS algorithms [20, 35, 31, 43], subset simulation (SuS) [2, 34, 42], line sampling (LS) [37, 38], directional sampling (DS) [16, 4], directional importance sampling (DIS) [21, 48], sequential directional importance sampling (SDIS) [12].

In this paper, we present an enhanced SDIS method. In SDIS, the failure probability is decomposed into a group of integrals, defined by magnifying the input variability. The first integral is estimated with MCS, while the subsequent ones are estimated with directional importance sampling. SDIS has been shown to be efficient for problems with low magnitude of failure probability, multiple failure domains, and many input variables [12]. However, the efficiency of SDIS depends on the initial magnification factor and the root-finding algorithm implemented to estimate the failure probability on every important direction. In this work, we enhance the performance of SDIS by the following modifications:

1. We note that the MCS estimator of the first integral in SDIS given in [12] is biased, and provide an unbiased estimator.
2. We discuss the efficiency of estimating the first integral with MCS in SDIS, and propose to estimate it with SuS.
3. We propose a Kriging-based active learning algorithm for finding roots within a narrow confidence interval on every important direction.

To evaluate the effect of these modifications, we compare the performance of the enhanced SDIS with the original SDIS and SuS on various benchmark reliability problems of different complexity. We find significant performance improvements for selected problems.

The layout of this paper is as follows. In section 2, we review the background of MCS, IS, DS and DIS methods. In Section 3, we present the enhanced SDIS algorithm, where the SDIS estimator, resampling technique, MCMC algorithm, the Kriging-based active learning root-finding technique, and the SuS method for estimating the first integral in SDIS are presented. In Section 4, several benchmarks are used to compare the performance of SDIS and SuS. The paper concludes with final remarks in Section 5.

2. Background

As is common in structural reliability [14], the failure probability in Eq. (1) is reformulated in standard normal space as

$$P_f = \int_{\mathbb{R}^n} I(G(\mathbf{u}) \leq 0) \varphi_n(\mathbf{u}) d\mathbf{u} = \mathbb{E}_{\varphi_n} [I(G(\mathbf{U}) \leq 0)], \quad (2)$$

where $\varphi_n(\mathbf{u})$ is the n -dimensional joint PDF of an independent standard normal random vector \mathbf{U} , and $G(\mathbf{u}) = g(\mathbf{T}^{-1}(\mathbf{u}))$ is the transformed LSF in

the standard normal space, in which \mathbf{T} is an isoprobabilistic transformation function [25].

MCS is the most straightforward and robust method to estimate the integral in Eq. (2). To implement it, one draws N samples $\{\mathbf{u}_i, i = 1, \dots, N\}$ from $\varphi_n(\mathbf{u})$, evaluates $I(G(\mathbf{u}_i) \leq 0)$, and uses the sample mean to estimate P_f as

$$P_f \approx \hat{P}_f = \frac{1}{N} \sum_{i=1}^N I(G(\mathbf{u}_i) \leq 0). \quad (3)$$

The MCS estimator in Eq. (3) is unbiased, and its coefficient of variation (CoV) is given by

$$\delta = \sqrt{\frac{1 - P_f}{NP_f}}. \quad (4)$$

With P_f in the order of 10^{-k} , MCS approximately requires 10^{k+2} samples to obtain an estimator with $\delta = 0.1$, which is infeasible for expensive computational models with low magnitude of failure probability. To reduce the computational cost, importance sampling (IS) reformulates the integral in Eq. (2) as

$$P_f = \int_{\mathbb{R}^n} I(G(\mathbf{u}) \leq 0) \frac{\varphi_n(\mathbf{u})}{h(\mathbf{u})} h(\mathbf{u}) d\mathbf{u} = \mathbb{E}_h [I(G(\mathbf{U}) \leq 0) W(\mathbf{U})], \quad (5)$$

where $h(\mathbf{u})$ is the IS density, and $W(\mathbf{u}) = \varphi_n(\mathbf{u})/h(\mathbf{u})$ is the importance weight. In IS, one draws a group of samples $\{\mathbf{u}_i, i = 1, \dots, N\}$ from $h(\mathbf{u})$, and P_f can be approximated as

$$P_f \approx \hat{P}_f = \frac{1}{N} \sum_{i=1}^N I(G(\mathbf{u}_i) \leq 0) W(\mathbf{u}_i). \quad (6)$$

The performance of IS depends on the choice of the IS density $h(\mathbf{u})$, and the optimal IS density is given by

$$h_{opt}(\mathbf{u}) = \frac{I(G(\mathbf{u}) \leq 0) \varphi_n(\mathbf{u})}{P_f}. \quad (7)$$

The estimator of Eq. (6) with IS density $h_{opt}(\mathbf{u})$ has zero variance. However, $h_{opt}(\mathbf{u})$ is not applicable in practice since it requires the knowledge of the

failure probability P_f .

Alternatively, the failure probability can be estimated in polar coordinates through a coordinate transformation of the outcome space of the standard normal distribution. In polar coordinates, one can express the failure probability as

$$P_f = \int_{\mathbb{S}^{n-1}} \int_0^\infty I(G(r\mathbf{a}) \leq 0) f_{\chi_n}(r) f_A(\mathbf{a}) dr d\mathbf{a} = \mathbb{E}_{f_{\chi_n}, f_A} [I(G(R\mathbf{A}) \leq 0)], \quad (8)$$

where \mathbf{a} is the direction and r is the radius; $f_{\chi_n}(r)$ is the PDF of radius, given by the χ distribution with n degrees-of-freedom, and $f_A(\mathbf{a})$ is the PDF of direction on the $n - 1$ dimensional unit hypersphere. In a similar manner to Eq. (5), the polar representation of the failure probability in Eq. (8) can be reformulated by IS as

$$P_f = \int_{\mathbb{S}^{n-1}} \int_0^\infty I(G(r\mathbf{a}) \leq 0) W(r, \mathbf{a}) h(r, \mathbf{a}) dr d\mathbf{a} = \mathbb{E}_h [I(G(R\mathbf{A}) \leq 0) W(R, \mathbf{A})], \quad (9)$$

where $h(r, \mathbf{a})$ is the joint IS density of radius and direction, $W(r, \mathbf{a}) = f_{\chi_n}(r) f_A(\mathbf{a}) / h(r, \mathbf{a})$ is the importance weight. The optimal zero-variance IS density in polar coordinates is given by

$$h_{opt}(r, \mathbf{a}) = \frac{I(G(r\mathbf{a}) \leq 0) f_{\chi_n}(r) f_A(\mathbf{a})}{P_f}. \quad (10)$$

As with Eq. (7), the optimal IS density in Eq. (10) cannot be implemented in practice. Alternatively, directional sampling (DS) makes use of the fact that one can reformulate the failure probability in Eq. (8) as [16]

$$\begin{aligned} P_f &= \int_{\mathbb{S}^{n-1}} \int_0^\infty I(G(r\mathbf{a}) \leq 0) f_{\chi_n}(r) dr f_A(\mathbf{a}) d\mathbf{a} \\ &= \int_{\mathbb{S}^{n-1}} \Pr(G(R\mathbf{a}) \leq 0) f_A(\mathbf{a}) d\mathbf{a} \\ &= \mathbb{E}_{f_A} [\Pr(G(R\mathbf{A}) \leq 0)], \end{aligned} \quad (11)$$

where the failure probability conditional on a specific direction \mathbf{a} can be

obtained by finding the roots of $G(r\mathbf{a}) = 0$ [48], i.e.,

$$\Pr(G(R\mathbf{a}) \leq 0) = \begin{cases} \sum_{j=1}^m (-1)^j F_{\chi_n}(r_j(\mathbf{a})), & \text{if } m \text{ is even} \\ 1 - F_{\chi_n}(r_m(\mathbf{a})) + \sum_{j=1}^{m-1} (-1)^j F_{\chi_n}(r_j(\mathbf{a})), & \text{if } m \text{ is odd} \end{cases} \quad (12)$$

where $F_{\chi_n}(\cdot)$ is the CDF of χ distribution with n degree-of-freedom, and $\{r_j(\mathbf{a}), j = 1, \dots, m\}$ are the roots of $G(r\mathbf{a}) = 0$ in direction \mathbf{a} .

To estimate P_f with DS, one first draws a group of directional vectors $\{\mathbf{a}_i, i = 1, \dots, N\}$ uniformly on the $n - 1$ dimensional unit hyper-sphere, and then evaluates the conditional failure probabilities $\Pr(G(R\mathbf{a}_i) \leq 0)$ by finding the roots of $G(r\mathbf{a}_i) = 0$ in each direction \mathbf{a}_i . The DS estimator is finally given by

$$P_f \approx \hat{P}_f = \frac{1}{N} \sum_{i=1}^N \Pr(G(R\mathbf{a}_i) \leq 0). \quad (13)$$

The above DS estimator is unbiased, but it is inefficient for high-dimensional problems since a large number of directions are required to sufficiently cover the $n - 1$ dimensional unit sphere, and a large portion of them may point towards the safe domain. To alleviate this problem, directional importance sampling (DIS) reformulates the DS estimator in Eq. (11) as

$$P_f = \int_{\mathbb{S}^{n-1}} \Pr(G(R\mathbf{a}) \leq 0) \frac{f_A(\mathbf{a})}{h(\mathbf{a})} h(\mathbf{a}) d\mathbf{a} = \mathbb{E}_h [\Pr(G(R\mathbf{A}) \leq 0) W(\mathbf{A})], \quad (14)$$

where $h(\mathbf{a})$ is the DIS density, and $W(\mathbf{a}) = f_A(\mathbf{a})/h(\mathbf{a})$ is the directional importance weight. The optimal DIS density in theory is given by

$$h_{opt}(\mathbf{a}) = \frac{\Pr(G(R\mathbf{a}) \leq 0) f_A(\mathbf{a})}{P_f}. \quad (15)$$

As with the optimal IS densities in Eqs. (7) and (10), the density $h_{opt}(\mathbf{a})$ in Eq. (15) cannot be used in practice. Recently, several adaptive methods have been proposed to design the DIS density [21, 40, 48], but they are only effective for low-to-moderate dimensional problems.

3. Enhanced sequential directional importance sampling

In this section, we introduce the enhanced SDIS algorithm. To make this paper self-contained, we also recap the resampling technique, MCMC algorithm as well as the parameter choice strategy implemented in [12]. The novel elements of the enhanced SDIS compared to the SDIS method of [12] are the unbiased MCS estimator of the first probability integral, discussed in Section 3.1, the root-finding algorithm presented in Section 3.5 and the SuS estimator of the first integral presented in Section 3.6.

3.1. Sequential directional importance sampling

In SDIS, a family of auxiliary failure probabilities $\{P_{\sigma_1}, \dots, P_{\sigma_M}\}$ are defined by magnifying the variability of the input random variables as

$$P_{\sigma_i} = \int_{\mathbb{R}^n} I(G(\sigma_i \mathbf{u}) \leq 0) \varphi_n(\mathbf{u}) d\mathbf{u} = \int_{\mathbb{S}^{n-1}} \Pr(G(\sigma_i R \mathbf{a}) \leq 0) f_A(\mathbf{a}) d\mathbf{a}, \quad (16)$$

where $\{\sigma_i, i = 1, \dots, M\}$, are magnification factors satisfying $1 = \sigma_M \leq \dots \leq \sigma_1$, and $G(\sigma_i \mathbf{u}) = G(\sigma_i r \mathbf{a})$ is the i -th auxiliary LSF.

By presetting an initial magnification factor σ_1 , the first auxiliary failure probability P_{σ_1} in SDIS is estimated with MCS. In this step, one draws samples from $\varphi_n(\mathbf{u})$ one-by-one until n_s (with $n_s \in [100, 200]$) samples in the inflated failure domain $F_{\sigma_1} = \{\mathbf{u} \in \mathbb{R}^n : G(\sigma_1 \mathbf{u}) \leq 0\}$ are generated. An estimate \hat{P}_{σ_1} of P_{σ_1} is given by

$$P_{\sigma_1} \approx \hat{P}_{\sigma_1} = \frac{n_s - 1}{N - 1}, \quad (17)$$

where N is the total number of samples drawn from $\varphi_n(\mathbf{u})$ until n_s failure samples are obtained. This is the unbiased estimator of P_{σ_1} in a Bernoulli process when a random number N of samples are drawn until a fixed number of n_s failure samples are obtained [22]. By contrast, the estimator n_s/N used in [12] is biased. An unbiased estimate of the variance of \hat{P}_{σ_1} is given by [18]

$$\text{Var}[\hat{P}_{\sigma_1}] \approx \frac{\hat{P}_{\sigma_1}(1 - \hat{P}_{\sigma_1})}{N - 2}. \quad (18)$$

A corresponding estimate of the CoV of \hat{P}_{σ_1} is

$$\delta_{\hat{P}_{\sigma_1}} \approx \sqrt{\frac{1 - \hat{P}_{\sigma_1}}{(N - 2)\hat{P}_{\sigma_1}}}. \quad (19)$$

In SDIS, the subsequent auxiliary failure probabilities $P_{\sigma_i} (i > 1)$ are expressed by DIS as

$$\begin{aligned} P_{\sigma_i} &= \int_{\mathbb{R}^n} I(G(\sigma_i \mathbf{u}) \leq 0) \varphi_n(\mathbf{u}) d\mathbf{u} \\ &= \int_{\mathbb{S}^{n-1}} \Pr(G(\sigma_i R\mathbf{a}) \leq 0) f_A(\mathbf{a}) d\mathbf{a} \\ &= P_{\sigma_{i-1}} \int_{\mathbb{S}^{n-1}} \frac{\Pr(G(\sigma_i R\mathbf{a}) \leq 0)}{\Pr(G(\sigma_{i-1} R\mathbf{a}) \leq 0)} \frac{\Pr(G(\sigma_{i-1} R\mathbf{a}) \leq 0) f_A(\mathbf{a})}{P_{\sigma_{i-1}}} d\mathbf{a} \quad (20) \\ &= P_{\sigma_{i-1}} \mathbb{E}_{h_{\sigma_{i-1}}} \left[\frac{\Pr(G(\sigma_i R\mathbf{a}) \leq 0)}{\Pr(G(\sigma_{i-1} R\mathbf{a}) \leq 0)} \right] \\ &= P_{\sigma_{i-1}} \mathbb{E}_{h_{\sigma_{i-1}}} [W_{i-1}(\mathbf{A})], \end{aligned}$$

where

$$h_{\sigma_{i-1}}(\mathbf{a}) = \frac{\Pr(G(\sigma_{i-1} R\mathbf{a}) \leq 0) f_A(\mathbf{a})}{P_{\sigma_{i-1}}} \quad (21)$$

is the optimal DIS density of the $i - 1$ -th auxiliary reliability problem, and

$$W_{i-1}(\mathbf{a}) = \frac{\Pr(G(\sigma_i R\mathbf{a}) \leq 0)}{\Pr(G(\sigma_{i-1} R\mathbf{a}) \leq 0)}. \quad (22)$$

is the directional importance weight. In this manner, the failure probability P_f is expressed as

$$P_f = P_{\sigma_1} \prod_{i=1}^{M-1} S_i, \quad (23)$$

where $S_i = \mathbb{E}_{h_{\sigma_i}} [W_i(\mathbf{A})]$ is the ratio between two adjacent auxiliary failure probabilities. It can be estimated by the sample mean of the directional importance weight $W_i(\mathbf{A})$ as

$$S_i \approx \hat{S}_i = \frac{1}{n_s} \sum_{k=1}^{n_s} \frac{\Pr(G(\sigma_{i+1} R\mathbf{a}_k) \leq 0)}{\Pr(G(\sigma_i R\mathbf{a}_k) \leq 0)}, \quad (24)$$

where $\{\mathbf{a}_k, k = 1, \dots, n_s\}$ are drawn from the DIS density $h_{\sigma_i}(\mathbf{a})$. The magnification factors $\sigma_i, i > 1$, are determined on the fly as detailed in Section 3.4.

Both $\Pr(G(\sigma_{i+1}R\mathbf{a}) \leq 0)$ and $\Pr(G(\sigma_i R\mathbf{a}) \leq 0)$ in Eq. (24) can be estimated following Eq. (12), i.e., by finding the roots of $G(\sigma_{i+1}r\mathbf{a}) = 0$ and $G(\sigma_i r\mathbf{a}) = 0$ in direction \mathbf{a} . In practice, one only needs to find the roots $\{r_{i+1,j}(\mathbf{a}), j = 1, \dots, m\}$ of $G(\sigma_{i+1}r\mathbf{a}) = 0$; the roots of $G(\sigma_i r\mathbf{a}) = 0$ in the same direction \mathbf{a} can be obtained by forcing $\sigma_{i+1}r_{i+1,j}(\mathbf{a})\mathbf{a} = \sigma_i r_{i,j}(\mathbf{a})\mathbf{a}$ for $j = 1, \dots, m$, as

$$r_{i,j}(\mathbf{a}) = \frac{\sigma_{i+1}r_{i+1,j}(\mathbf{a})}{\sigma_i}, j = 1, \dots, m. \quad (25)$$

3.2. Resampling algorithm

In the SDIS procedure, one needs to sample a directional vector \mathbf{a} from the DIS density function $h_{\sigma_i}(\mathbf{a}) = \Pr(G(\sigma_i R\mathbf{a}) \leq 0) f_A(\mathbf{a})/P_{\sigma_i}$. To draw directional vectors \mathbf{a} from the first DIS density $h_{\sigma_1}(\mathbf{a})$, one can apply a polar coordinate transformation to the n_s failure samples $\{\mathbf{u}_i, i = 1, \dots, n_s\}$ following $h_{\sigma_1}(\mathbf{u}) = I(G(\sigma_1\mathbf{u}) \leq 0) \varphi_n(\mathbf{u})/P_{\sigma_1}$ obtained in the first step when estimating P_{σ_1} with MCS. Indeed, for a sample \mathbf{u} drawn from $h_{\sigma_i}(\mathbf{u})$ in Cartesian coordinates, the corresponding polar representation $\{\mathbf{a}, r\}$ follow the following joint IS density due to transformation of variables:

$$h_{\sigma_i}(r, \mathbf{a}) = \frac{I(G(\sigma_i r\mathbf{a}) \leq 0) f_{\chi_n}(r) f_A(\mathbf{a})}{P_{\sigma_i}}. \quad (26)$$

The DIS density $h_{\sigma_i}(\mathbf{a})$ is simply the marginal distribution of \mathbf{a} , namely

$$h_{\sigma_i}(\mathbf{a}) = \int_0^\infty h_{\sigma_i}(r, \mathbf{a}) dr = \frac{\Pr(G(\sigma_i R\mathbf{a}) \leq 0) f_A(\mathbf{a})}{P_{\sigma_i}}. \quad (27)$$

As a result, by normalizing samples \mathbf{u} drawn from IS density $h_{\sigma_i}(\mathbf{u})$ in Cartesian coordinates, one obtains the corresponding directional vector $\mathbf{a} = \mathbf{u}/\|\mathbf{u}\|$ that follows the DIS density $h_{\sigma_i}(\mathbf{a})$ in polar coordinates.

In the subsequent steps, a resample-move scheme is applied to draw samples from $h_{\sigma_i}(\mathbf{a}) (i > 1)$. One first resamples a group of initial samples from existing samples obtained from the previous sampling step and then moves these samples to regions of high probability mass of $h_{\sigma_i}(\mathbf{a})$ by applying MCMC sampling algorithm with invariant distribution $h_{\sigma_i}(\mathbf{a})$. However, evaluation of the acceptance probability in classical Metropolis-

Hastings (M-H) algorithms, as detailed in Section 3.3, requires evaluation of the target distribution $h_{\sigma_i}(\mathbf{a})$ and, hence, the conditional failure probability $\Pr(G(\sigma_i R\mathbf{a}) \leq 0)$, at the candidate state. Each evaluation of this probability requires finding the roots of $G(\sigma_i r\mathbf{a}) = 0$. To avoid this problem, we suggest to apply a resample-move scheme for drawing samples $\{\mathbf{u}_k, k = 1, \dots, n_s\}$ from the distribution $h_{\sigma_i}(\mathbf{u}) = I(G(\sigma_i \mathbf{u}) \leq 0) \varphi_n(\mathbf{u}) / P_{\sigma_i}$. The directional vector following $h_{\sigma_i}(\mathbf{a})$ is then obtained by normalizing the samples drawn from $h_{\sigma_i}(\mathbf{u})$, namely, $\{\mathbf{a}_k = \mathbf{u}_k / \|\mathbf{u}_k\|, k = 1, \dots, n_s\}$.

To draw initial samples from $h_{\sigma_i}(\mathbf{u})$, one can apply the following resampling algorithm:

1. Resampling of direction: select n_a samples $\{\mathbf{a}_k, k = 1, \dots, n_s\}$ with replacement from the existing directional samples following $h_{\sigma_{i-1}}(\mathbf{a})$ randomly with probability assigned to each sample proportional to the importance weight $W_{i-1}(\mathbf{u})$.

2. Resampling of radius: For each directional vector $\mathbf{a}_k (k = 1, \dots, n_s)$ obtained in step 1, generate a random sample of the radius $r(\mathbf{a}_k)$ following the truncated χ_n distribution $f_{\chi_n}(r|F_{\mathbf{a}_k})$, where $F_{\mathbf{a}_k} = \{r \in \mathbb{R} : G(\sigma_i r\mathbf{a}_k) \leq 0\}$ is the failure domain in direction \mathbf{a}_k , given by

$$F_{\mathbf{a}_k} = \begin{cases} r \in \bigcup_{j \in \{1, 3, \dots, m-1\}} [r_{i,j}(\mathbf{a}_k), r_{i,j+1}(\mathbf{a}_k)], & \text{if } m \text{ is even} \\ r \in \bigcup_{j \in \{1, 3, \dots, m-2\}} [r_{i,j}(\mathbf{a}_k), r_{i,j+1}(\mathbf{a}_k)] \cup [r_{i,m}(\mathbf{a}_k), +\infty], & \text{if } m \text{ is odd} \end{cases}$$

The resampled sample pairs $\{\mathbf{a}_k, r(\mathbf{a}_k), k = 1, \dots, n_s\}$ follow the joint IS density function $h_{\sigma_i}(\mathbf{a}, r)$ asymptotically, and hence, the corresponding samples in Cartesian coordinates $\{\mathbf{u}_k = \mathbf{a}_k r(\mathbf{a}_k), k = 1, \dots, n_s\}$ follow $h_{\sigma_i}(\mathbf{u})$ asymptotically.

3.3. MCMC algorithm

Following the resampling step, MCMC sampling is applied to generate directional samples following $h_{\sigma_i}(\mathbf{a})$. As discussed in Section 3.2, this is achieved through first generating samples $\{\mathbf{u}_k, k = 1, \dots, n_s\}$ from $h_{\sigma_i}(\mathbf{u})$ using as seeds the Cartesian samples obtained in the resampling step, and then transforming the generated samples to directional samples, i.e., applying $\{\mathbf{a}_k = \mathbf{u}_k / \|\mathbf{u}_k\|, k = 1, \dots, n_s\}$.

For each seed $\{\mathbf{u}_k, k = 1, \dots, n_s\}$ obtained in the resampling step, one simulates a Markov chain of length l independently with stationary distribution

$h_{\sigma_i}(\mathbf{u})$ based on the M-H algorithm as follows:

1. Select a seed \mathbf{u}_t , and set $t = 0$.
2. Generate a random candidate sample pair \mathbf{u}' from the proposal distribution $q_{\sigma_i}(\mathbf{u}'|\mathbf{u}_t)$, and evaluate the model response $G(\sigma_i\mathbf{u}')$.
3. Calculate the acceptance probability

$$\alpha = I(G(\sigma_i\mathbf{u}') \leq 0) \min \left(1, \frac{\varphi_n(\mathbf{u}')q(\mathbf{u}_t|\mathbf{u}')}{\varphi_n(\mathbf{u}_t)q(\mathbf{u}'|\mathbf{u}_t)} \right). \quad (28)$$

4. Generate a random number $w \in [0, 1]$, and determine the next state pair as

$$\mathbf{u}_{t+1} = \begin{cases} \mathbf{u}_t & \text{if } w \geq \alpha \\ \mathbf{u}' & \text{if } w < \alpha \end{cases}; \quad (29)$$

5. Set $t = t + 1$, and go back to step 2 until the target length $l = 5$ is reached.

In SDIS, the conditional sampling (CS) method [34] is applied, in which the proposal distribution $q_{\sigma_i}(\mathbf{u}'|\mathbf{u}_t)$ is selected as the multivariate standard Gaussian density conditional on the current state \mathbf{u}_t

$$\mathbf{u}' = \rho_{\mathbf{u}}\mathbf{u}_t + \sqrt{1 - \rho_{\mathbf{u}}^2}\boldsymbol{\xi}, \quad (30)$$

where $\boldsymbol{\xi} \in \mathbb{R}^n$ is a realization of an n -dimensional independent standard normal random vector, and $\rho_{\mathbf{u}}$ is the correlation coefficient between \mathbf{u}_t and \mathbf{u}' . The correlation parameter $\rho_{\mathbf{u}}$ is determined adaptively to ensure that the acceptance probability α is close to a near-optimal value 44% [34].

With the above proposal, the MCMC acceptance probability in Eq. (28) becomes

$$\alpha = I(G(\sigma_i\mathbf{u}') \leq 0). \quad (31)$$

To reduce the effect of the transient period of the simulated Markov chain and reduce the correlation between Markov Chain states, we discard the first l samples from every Markov chain. This means that only the last state of each Markov chain is retained, which is expected to follow the target distribution $h_{\sigma_i}(\mathbf{u})$ closely.

3.4. Choice of parameters for SDIS

There are several user-specified parameters in SDIS, including the initial magnification factor σ_1 , the number of important directional vectors per level

n_s , and the Markov chain length l . Based on our previous work [12] and numerical experiments, we suggest setting $\sigma_1 = 3, n_s \in [100, 200], l = 5$.

The magnification factor in the subsequent steps $\{\sigma_i, i > 1\}$ can be determined on the fly by forcing the CoV of the directional importance weight to adhere to a target value δ_{target} , which corresponds to solving the following optimization problem [36]:

$$\sigma_i = \underset{\sigma_i \in [1, \sigma_{i-1}]}{\operatorname{argmin}} |\hat{\delta}_{W_i} - \delta_{\text{target}}|, (i \geq 2), \quad (32)$$

where $\hat{\delta}_{W_i}$ is the CoV of the importance weight $\{W_i(\mathbf{a}_j), j = 1, \dots, n_s\}$. We use $\delta_{\text{target}} = 1.5$ for the target CoV.

Assuming that directional vectors drawn from $h_{\sigma_i}(\mathbf{a})$ are independent from samples drawn at other steps $h_{\sigma_j}(\mathbf{a}) (i \neq j)$, and that the directional vectors at each level drawn from $h_{\sigma_i}(\mathbf{a})$ are independent from each other, the CoV of the SDIS estimator can be approximated by [12]

$$\delta_{\hat{P}_f} \approx \sqrt{\delta_{\hat{P}_{\sigma_1}}^2 + \sum_{i=1}^{M-1} \delta_{\hat{S}_i}^2}, \quad (33)$$

where $\delta_{\hat{P}_{\sigma_1}}$ is the CoV of \hat{P}_{σ_1} , and $\delta_{\hat{S}_i}$ is the CoV of S_i , which is given by

$$\delta_{\hat{S}_i} \approx \frac{\delta_{W_i(\mathbf{A})}}{\sqrt{n_s}}. \quad (34)$$

$\delta_{W_i(\mathbf{A})}$ denotes the CoV of the importance weight $W_i(\mathbf{A})$, and it is estimated from the existing samples $\{W_i(\mathbf{a}_i), i = 1, \dots, n_s\}$. Note that $\delta_{\hat{P}_f}$ underestimates the true CoV of \hat{P}_f due to the independence assumption.

3.5. Root-finding algorithm

To estimate the conditional probability $\Pr(G(\sigma_i R \mathbf{a}) \leq 0)$ in Eq. (12), one needs to find the roots of $G(\sigma_i r \mathbf{a}) = 0$ along direction \mathbf{a} . In [12], the trust-region dogleg algorithm (“fsolve” function in Matlab) is applied. However, it can only find one root along each direction. To address this issue, we introduce a Kriging-based active learning algorithm for identifying the roots in this section.

Since the radius r follows the χ_n distribution, we limit the search domain

on the radius to the following interval

$$[r^-, r^+] = [F_{\chi_n}^{-1}(\alpha/2), F_{\chi_n}^{-1}(1 - \alpha/2)], \quad (35)$$

where α is a small positive constant. As $(1-\alpha)\%$ probability mass of the PDF of radius concentrates on this interval, we can obtain an accurate estimation of the failure probability $\Pr(G(\sigma_i R \mathbf{a}) \leq 0)$ by finding the roots of $G(\sigma_i r \mathbf{a}) = 0$ within this interval in direction \mathbf{a} . In Table 1, a series of intervals are listed by varying the input dimension n for $\alpha = 10^{-10}$. Although the lower bound and upper bound increase with n , it is observed that the interval width converges to a constant as $n \rightarrow \infty$. This is due to the fact that the χ_n distribution is approximately normal as $n \rightarrow \infty$ with variance $1/2$, which is independent of n [28]. Therefore, to find the roots along each direction we only need to construct an accurate Kriging model within a narrow interval. In SDIS, the roots of $G(\sigma_i r \mathbf{a}) = 0$ will be used to compute the roots of $G(\sigma_{i+1} r \mathbf{a}) = 0$ via the relationship in Eq. (25). The roots of the first few auxiliary LSFs $G(\sigma_i r \mathbf{a}) = 0 (i = 1, \dots)$ may be smaller than the lower bound $F_{\chi_n}^{-1}(\alpha/2)$ given in Eq. (35). To ensure that all roots of $G(\sigma_i r \mathbf{a}) = 0$ are contained in the interval, we apply a very conservative lower bound $r^- = F_{\chi_n}^{-1}(\alpha/2)/\sigma_i$ in practice.

Table 1: Interval defining the search domain on the radius for $\alpha = 10^{-10}$ and different dimension n

Dimension n	Lower bound r^-	Upper bound r^+	Width
10	0.21	8.35	8.14
10^2	5.80	14.84	9.04
10^3	27.16	36.29	9.13
10^4	95.46	104.60	9.14
10^5	311.67	320.81	9.15
10^6	995.43	1004.57	9.15

Given an initial training set $\{\mathbf{X}, \mathbf{Y}\}$ on direction \mathbf{a} , where $\mathbf{X} = [r^{(1)}, \dots, r^{(M)}]^T$, $\mathbf{Y} = [G(\sigma_i r^{(1)} \mathbf{a}), \dots, G(\sigma_i r^{(M)} \mathbf{a})]^T$, we construct a 1-dimensional Kriging model as [30]

$$\hat{Y}(r) \sim \mathcal{N}(\mu(r), s^2(r)), \quad (36)$$

where $\mu(r)$ and $s^2(r)$ are the Kriging mean and variance respectively. In the current work, the Matérn 5/2 correlation function is used. More details of

the Kriging model are provided in Appendix A.

We then select informative samples to refine the Kriging model sequentially. We apply the learning function developed in [47] to select the optimal next point, which is defined as follows:

$$\mathbf{L}(r) = \begin{cases} \mathbb{E}[\max(\hat{Y}(r), 0)], & \text{if } \mu(r) < 0 \\ \mathbb{E}[\max(-\hat{Y}(r), 0)], & \text{if } \mu(r) > 0 \end{cases} \quad (37)$$

It measures the average distance of the predicted response to the limit state surface $G(\sigma_i r \mathbf{a}) = 0$ when it is misclassified. The analytical expression of this function is given by [47]

$$\mathbf{L}(r) = -\text{sgn}(\mu(r)) \mu(r) \Phi\left(-\text{sgn}(\mu(r)) \frac{\mu(r)}{s(r)}\right) + s(r) \varphi\left(\frac{\mu(r)}{s(r)}\right), \quad (38)$$

where $\Phi(\cdot)$ and $\varphi(\cdot)$ are the CDF and PDF of the standard normal distribution respectively, and $\text{sgn}(\cdot)$ is the sign function. The convergence criterion used in this work is $\max(\mathbf{L}(r))/|\bar{y}| < \epsilon$, where $\max(\mathbf{L}(r))$ is the maximum of $\mathbf{L}(r)$, $|\bar{y}|$ is the mean of the absolute value of the model response in the training set and ϵ is a user-specified constant. A small ϵ will yield more accurate roots but requires more model evaluations, and vice versa. Here we set $\epsilon = 5 \times 10^{-4}$.

In the current work, we construct a Kriging model with a few initial radius samples in every direction. The initial sample size (3 or 4) is determined heuristically, depending on the degree of nonlinearity of the problem at hand. The first radius sample is the origin $r^{(1)} = 0$, which is shared by all directions; the second sample is the radius of the failure sample \mathbf{u} that defines the current direction, namely, $r^{(2)} = \|\mathbf{u}\|$; the third sample is determined as

$$r^{(3)} = \begin{cases} (r^- + r^{(2)})/2, & \text{if } |r^{(2)} - r^+| < |r^+ - r^-|/3, \\ (r^+ + r^{(2)})/2, & \text{else.} \end{cases} \quad (39)$$

With the setting in Eq. (39), we put the third radius sample at the midpoint between the second one and either the lower bound r^- or the upper bound, depending on the distance $|r^{(2)} - r^+|$. If the average sample size of the Kriging model after active learning along previous n_{s1} directions is greater than 4, we turn to train the Kriging model along the remaining $n_s - n_{s1}$ directions with 4 initial radius samples. The location of the fourth radius

sample is set to

$$r^{(4)} = \begin{cases} (r^{(3)} + r^{(2)})/2, & \text{if } |r^{(2)} - r^+| < |r^+ - r^-|/3 \text{ and } G(\sigma_i r^{(3)} \mathbf{a}) > 0, \\ (r^- + r^{(3)})/2, & \text{if } |r^{(2)} - r^+| < |r^+ - r^-|/3 \text{ and } G(\sigma_i r^{(3)} \mathbf{a}) < 0, \\ (r^- + r^{(2)})/2, & \text{else} \end{cases} \quad (40)$$

In Figs. 1, 2 and 3, we present three examples of the active learning Kriging model for finding the root of $G(\sigma_1 r \mathbf{a}) = 0$ in the Example of Section 4.3 in the interval $[0.0362, 8.0574]$. The figures show that the Kriging model can find all roots in these cases, and the enriched samples are quite close to the failure boundary, thereby refining the accuracy of the roots.

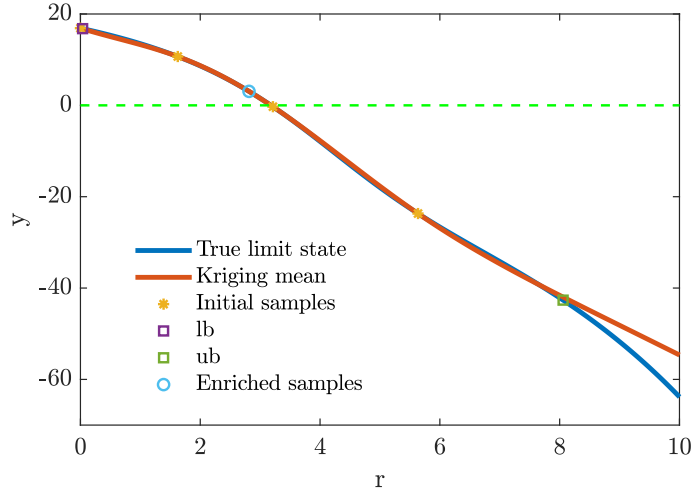


Figure 1: Active learning Kriging model for finding root (one root case) in interval $[0.0362, 8.0574]$.

3.6. The efficiency of estimating P_{σ_1}

In SDIS, the efficiency of estimating P_{σ_1} with MCS in the first step depends on the initial magnification factor σ_1 , which is set to 3 in [12, 39] empirically. For most problems, this setting is efficient for generating failure samples lying in F_{σ_1} . To further illustrate its effectiveness, we consider three different types of limit state surfaces in 2-dimensional space, depicted in Fig. 4. For all the three cases, i.e., linear, concave and convex, the corresponding auxiliary limit state surfaces $G(\sigma \mathbf{u})$ are much closer to the origin compared

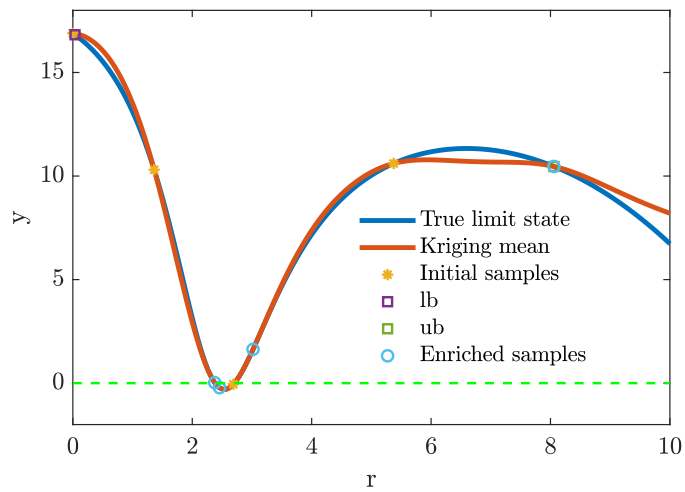


Figure 2: Active learning Kriging model for finding roots (two roots case) in interval $[0.0362, 8.0574]$.

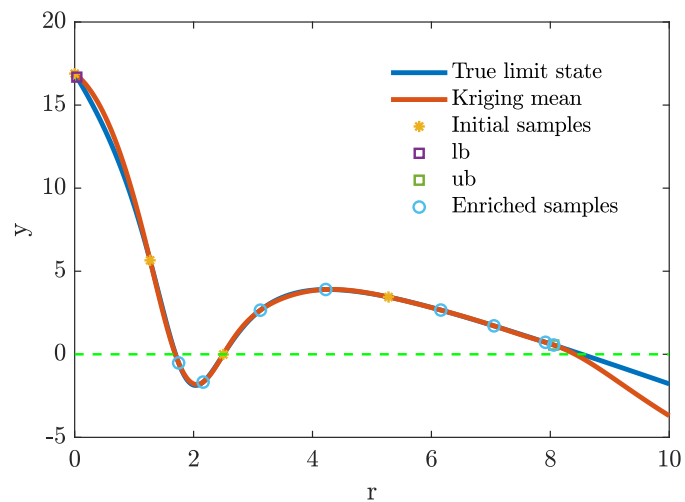


Figure 3: Active learning Kriging model for finding roots (three roots case) in interval $[0.0362, 8.0574]$.

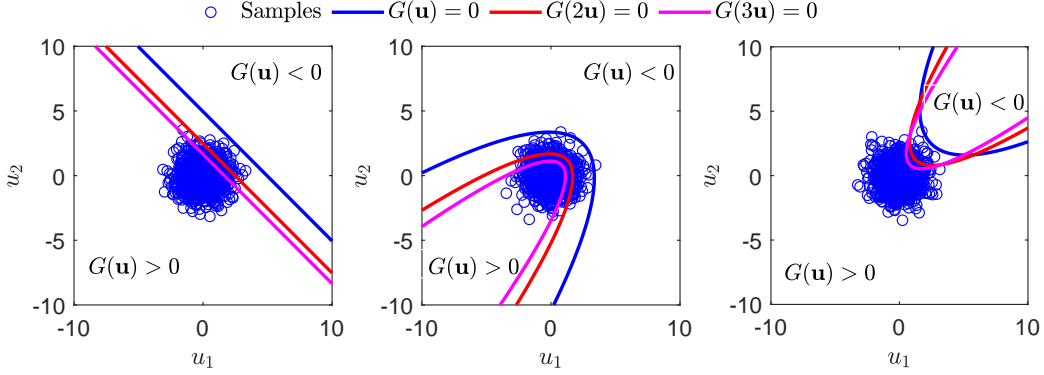


Figure 4: 1000 MCS samples drawn from standard normal PDF $\varphi_2(\mathbf{u})$ vs three types of limit states (left: linear; middle: concave; right: convex)

to the true ones, and one can obtain a group of failure samples lying in $F_{\sigma_1} = \{\mathbf{u} \in \mathbb{R}^n : G(\sigma_1 \mathbf{u}) \leq 0\}$ efficiently with MCS by drawing samples from $\varphi_2(\mathbf{u})$.

However, for problems with extremely low magnitude of failure probability or with a very narrow (e.g., island-shape) failure domain, only a small portion of the MCS population will reside in the failure domain F_{σ_1} . In Fig. 5, we present such an example, in which case MCS is inefficient for estimating P_{σ_1} . To address this problem, we suggest introducing another family of intermediate failure events $G(\sigma_1 \mathbf{u}) \leq b_j$ by modifying the failure threshold [11, 45]. In other words, we estimate P_{σ_1} with SuS. When $10n_s$ samples have been generated from $\varphi_n(\mathbf{u})$ one-by-one before n_s failure samples are obtained, we turn to estimate P_{σ_1} with SuS, which gives

$$P_{\sigma_1} = \prod_{j=1}^s \Pr(\mathbf{U} \in F_{\sigma_1, b_j} | \mathbf{U} \in F_{\sigma_1, b_{j-1}}), \quad (41)$$

where $F_{\sigma_1, b_j} = \{\mathbf{u} \in \mathbb{R}^n : G(\sigma_1 \mathbf{u}) \leq b_j\}$ are intermediate failure domains, and $\infty = b_0 > b_1 > \dots > b_s = 0$ are the corresponding intermediate failure thresholds. The thresholds $b_j (j = 1, \dots, s)$ are set as the p_0 -percentiles (we set $p_0 = 0.1$ in this study) of the limit-state function values $\{G(\sigma_1 \mathbf{u}_i), i = 1, \dots, n_s\}$, in which \mathbf{u}_i are sampled from $\varphi_n(\mathbf{u})$ in the initial step $j = 1$ with crude Monte Carlo, and from the IS density $h_{\sigma_1, b_j}(\mathbf{u}) \propto I(G(\sigma_1 \mathbf{u}) \leq b_j) \varphi_n(\mathbf{u})$ in steps $j = 2, \dots, s$ by MCMC through application of the adaptive conditional sampling algorithm [34]. In the last step of SuS, we obtain a group of failure

samples in $F_{\sigma_1} = \{\mathbf{u} \in \mathbb{R}^n : G(\sigma_1 \mathbf{u}) \leq 0\}$ drawn from the last IS density $h_{\sigma_1}(\mathbf{u}) \propto I(G(\sigma_1 \mathbf{u}) \leq 0) \varphi_n(\mathbf{u})$. By normalizing these samples, i.e., by applying $\mathbf{a} = \mathbf{u}/\|\mathbf{u}\|$, one can obtain a group of directional vectors following the first DIS density $h_{\sigma_1}(\mathbf{a})$. An estimate of the CoV of the SuS estimator of P_{σ_1} is given in [2].

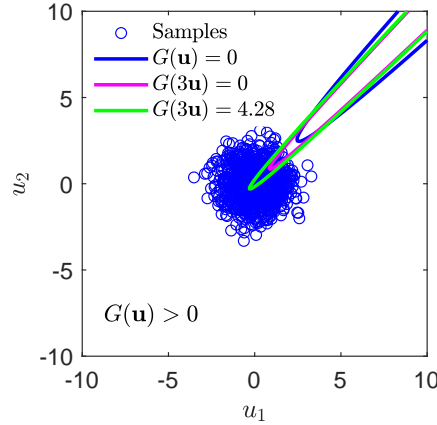


Figure 5: 1000 samples drawn from standard normal PDF vs a special LSF with narrow failure domain. The probability of a sample to fall into the inflated failure domain $F = \{\mathbf{u} \in \mathbb{R}^n : G(3\mathbf{u}) \leq 0\}$ is 0.014.

Remark 1. *The SuS estimator P_{σ_1} in Eq. (41) is biased due to the correlation between the estimates of the conditional probabilities $\Pr(\mathbf{U} \in F_{\sigma_1, b_j} | \mathbf{U} \in F_{\sigma_1, b_{j-1}})$ as well as the adaptive estimation of the intermediate failure domains $F_{\sigma_1, b_j} = \{\mathbf{u} \in \mathbb{R}^n : G(\sigma_1 \mathbf{u}) \leq b_j\}$ [34, 8]. However, this bias is small compared to the CoV of the estimator, hence it is not deemed critical.*

3.7. Summary of enhanced SDIS

The enhanced SDIS algorithm is summarized as follows:

1. Initialize: Set the initial magnification factor $\sigma_1 = 3$, the length of each Markov chain $l = 5$ and the number of the important directions per level $n_s (n_s \in [100, 200])$. Set $k = 1$.
2. Estimate the first auxiliary failure probability \hat{P}_{σ_1} with MCS or SuS and determine the directional samples following $h_{\sigma_1}(\mathbf{a})$ in terms of the failure samples $\{\mathbf{u}_i, i = 1, \dots, n_s\}$ through applying $\{\mathbf{a}_i = \mathbf{u}_i / \|\mathbf{u}_i\|, i = 1, \dots, n_s\}$.
3. Find the roots in the n_s important directions $\{\mathbf{a}_i, i = 1, \dots, n_s\}$ with active learning Kriging model.

4. Determine the next magnification factor σ_{k+1} by solving the optimization problem in Eq. (32).
5. Calculate the ratio \hat{S}_k between two adjacent auxiliary failure probabilities $P_{\sigma_{k+1}}$ and P_{σ_k} with Eq. (24)
6. Resample and move: Apply the resample and move algorithm introduced in Sections 3.2 and 3.3 to draw a group of samples $\{\mathbf{a}_i, i = 1, \dots, n_s\}$ following $h_{\sigma_{k+1}}(\mathbf{a})$.
7. Set $k = k + 1$, and go back to step 3 until $\sigma_{k+1} = 1$.
8. Calculate the final failure probability as

$$\hat{P}_f = \hat{P}_{\sigma_1} \prod_{i=1}^k \hat{S}_i. \quad (42)$$

4. Numerical examples

In this section, the effectiveness of the enhanced SDIS is investigated on several benchmarks. We compare it to SuS [1, 34] and standard SDIS [12] in terms of the relative efficiency with respect to crude MCS, a concept that is borrowed from statistics [32, 9]. This relative efficiency measure is defined as follows:

$$\text{relEff}(\hat{P}_f) := \frac{P_f(1 - P_f)}{\text{MSE}(\hat{P}_f)\text{Cost}(\hat{P}_f)}. \quad (43)$$

P_f is the failure probability reference value obtained with MCS or analytically. The mean square error $\text{MSE}(\hat{P}_f) = (P_f - \mathbb{E}[\hat{P}_f])^2 + \text{Var}(\hat{P}_f)$ accounts for both the bias and variance of the estimator. $\text{Cost}(\hat{P}_f)$ denotes the number of total model evaluations. In all numerical examples, we run both SuS and SDIS independently for 300 times to estimate the bias and variance of both estimators.

In all examples, the parameters of the enhanced SDIS and the standard SDIS [12] are set to $\sigma_1 = 3, n_s = 150, l = 5$. In SuS, the sample size per level is set to 1000, and the intermediate failure probability is set to 0.1. The Matlab package of enhanced SDIS and standard SDIS is available at <https://github.com/KaiChengDM/Enhanced-SDIS/tree/main> and <https://github.com/KaiChengDM/SDIS>. The SuS package used in this work for comparison is available at https://github.com/ERA-Software/Overview/tree/main/Reliability%20Analysis%20Tools/3.%20Subset%20Simulation/SuS_Matlab.

4.1. Two-dimensional example with multiple failure domains

In this example, we investigate the performance of the enhanced SDIS with the two-dimensional LSF adapted from [27]:

$$G(\mathbf{x}) = 5 \left(4 - 2.1x_1^2 + \frac{x_1^4}{3} \right) x_1^2 + 5x_1x_2 + 10(x_2^2 - 1)x_2^2 + 2.6, \quad (44)$$

where x_1 and x_2 are independent normal random variables with zero mean and standard deviation 0.05 and 0.18, respectively. We transform the LSF in Eq. (44) into standard normal space via isoprobabilistic transformation. The MCS reference value of failure probability with 10^8 samples is $P_f = 3.71 \times 10^{-5}$.

Fig. 6 depicts the limit state surface and a specific run of the enhanced SDIS for estimating the failure probability. It shows that the first auxiliary limit state surface $G(3\mathbf{u}) = 0$ is much closer to the origin compared to the true one. However, we only obtain 17 failure samples from the MCS population of size $10n_s$ drawn from standard normal PDF $\varphi_2(\mathbf{u})$, and SuS is applied to estimate P_{σ_1} in this case. In order to obtain n_s failure samples in the intermediate failure domain $F_{\sigma_1, b_1} = \{\mathbf{u} \in \mathbb{R}^n : G(\sigma_1\mathbf{u}) \leq b_1\}$, the failure threshold is set to $b_1 = 0.415$, and we obtain an estimate $\hat{P}_{\sigma_1} = 0.012$ with only one intermediate step in SuS. Then, we estimate the ratio $\hat{S}_1 = P_f/P_{\sigma_1}$, and a convergent estimator is obtained with only one additional step. The final estimate of failure probability is given by $\hat{P}_f = \hat{P}_{\sigma_1}\hat{S}_1$.

The reliability analysis results of the standard and enhanced SDIS and SuS are listed in Table 2, in which the mean of failure probability $\mathbb{E}(\hat{P}_f)$, the mean of the approximated CoV $\mathbb{E}(\hat{\delta}_{\hat{P}_f})$, the empirical CoV of the failure probability $\delta(\hat{P}_f)$, the mean of the total model evaluations $\mathbb{E}(N_t)$, and the relEff defined in Eq. (43) are provided. The approximated CoV of the enhanced SDIS is obtained by Eq. (33), and that of SuS is obtained by assuming independence of the estimates of the conditional probabilities in different level [2, 34]. The empirical CoV of the failure probability $\delta(\hat{P}_f)$ is obtained by repeating the entire analysis 300 times, hence this is the more realistic estimate of the CoV and is used to evaluate the relEff.

Since the enhanced SDIS requires fewer intermediate steps, one can see that it provides much more robust results with fewer model evaluations than SuS, and the relative efficiency relEff of the enhanced SDIS is one magnitude larger than that of SuS. Additionally, it is found that the approximated

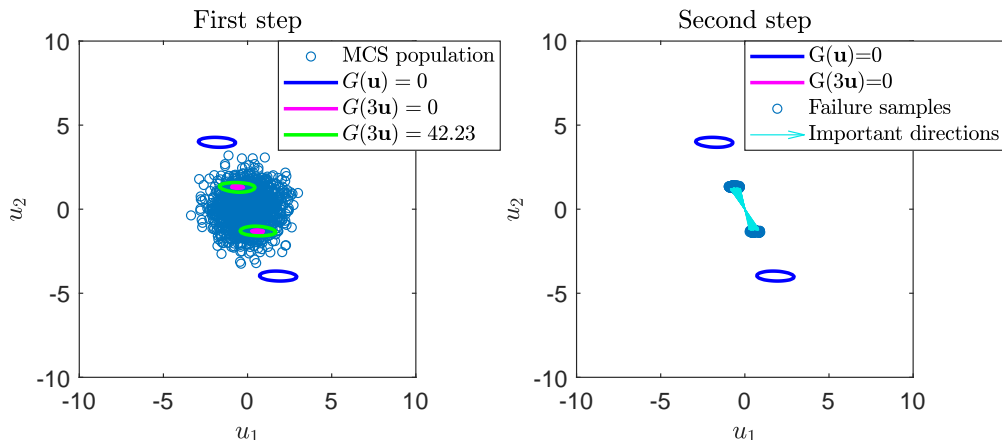


Figure 6: Samples, important directions and intermediate LSFs of SDIS in standard normal space in problem 4.1.

CoVs of both methods underestimate the true ones due to the independence assumption. In this problem, standard SDIS is inefficient since the standard root finding algorithm implemented used within this method can only find one root in every important direction, and the estimator is severely biased.

Table 2: Reliability analysis results for example 4.1 (Reference value: $P_f = 3.71 \times 10^{-5}$)

Method	$\mathbb{E}(\hat{P}_f)$	$\mathbb{E}(\delta_{\hat{P}_f})$	$\delta(\hat{P}_f)$	$\mathbb{E}(N_t)$	relEff
SuS	3.66×10^{-5}	0.30	0.37	5232	37.78
Enhanced SDIS	3.77×10^{-5}	0.15	0.17	3491	255.49
Standard SDIS	5.09×10^{-6}	0.11	0.12	1249	2.89

4.2. Two-dimensional metaball function

We consider the metaball LSF [7]:

$$G(\mathbf{u}) = \frac{30}{\left(\frac{4(u_1+2)^2}{9} + \frac{u_2^2}{25}\right)^2 + 1} + \frac{20}{\left(\frac{(u_1-2.5)^2}{4} + \frac{(u_2-0.5)^2}{25}\right)^2 + 1} - 5,$$

where u_1 and u_2 are standard normal random variables. The reference value of the failure probability obtained by MCS with 10^8 samples is $P_f = 1.12 \times 10^{-5}$.

Fig. 7 depicts the limit state surface and a specific run of the enhanced SDIS for estimating the failure probability in this example. Although there is only one failure domain, the failure boundary is irregular and highly nonlinear. In the enhanced SDIS, the first auxiliary limit state surface $G(3\mathbf{u}) = 0$ is much closer to the origin than the true one, and the first auxiliary failure probability is readily estimated with MCS. The $n_s = 150$ failure samples in the MCS population define n_s directional vectors $\{\mathbf{a}_i = \mathbf{u}_i / \|\mathbf{u}_i\|, i = 1, \dots, n_s\}$ following the first DIS density $h_{\sigma_1}(\mathbf{a})$ in the enhanced SDIS. By finding the roots along these directions with the Kriging model, we obtain an estimate \hat{S}_1 of S_1 in Eq. (24). Furthermore, σ_2 obtained by solving the optimization problem in Eq. (32) reduces to 1 directly. Hence, one obtains a convergent estimation of failure probability with only one intermediate step in the enhanced SDIS. By contrast, SuS gives poor result since the samples in the intermediate steps tend to be trapped in a local failure domain for this example [7, 39].

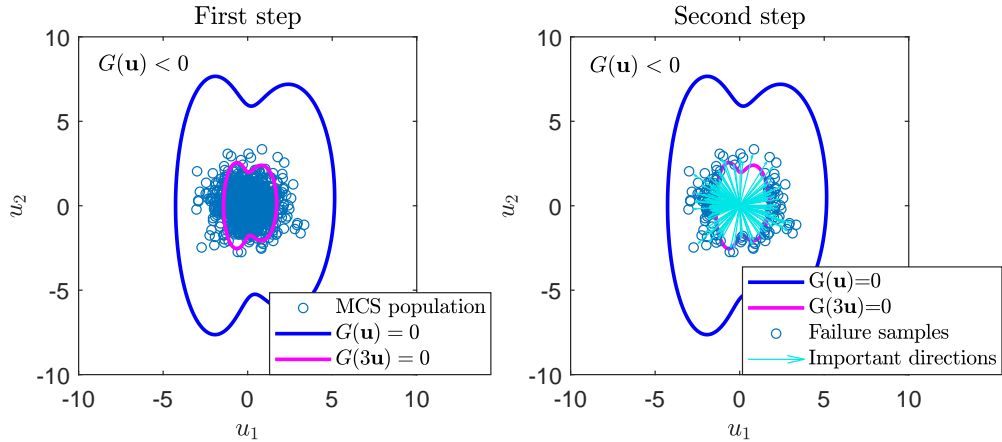


Figure 7: Samples, important directions and intermediate LSFs of SDIS in problem 4.2.

Table 3: Reliability analysis results for example 4.1 (Reference value: $P_f = 1.12 \times 10^{-5}$)

Method	$\mathbb{E}(\hat{P}_f)$	$\mathbb{E}(\delta_{\hat{P}_f})$	$\delta(\hat{P}_f)$	$\mathbb{E}(N_t)$	relEff
SuS	1.14×10^{-5}	0.46	2.93	7751	1.29
Enhanced SDIS	1.07×10^{-5}	0.13	0.15	3562	1163.58
Standard SDIS	1.14×10^{-5}	0.14	0.16	3641	982.85

The results are summarized in Table 3. Both the standard and enhanced SDIS provide much more robust results with less model evaluations compared to SuS. Indeed, SuS degenerates to crude Monte Carlo simulation in this challenging problem. However, this problem has been specifically designed in [7] to cause problems for SuS, so the comparison may be unfair. Since there is only one root in every important direction, the standard SDIS is comparable to the enhanced SDIS in this example.

4.3. Nonlinear oscillator

We test the performance of the enhanced SDIS method by assessing the reliability of a two-degree-of-freedom primary–secondary system under a white noise base acceleration [29, 5]. The system failure occurs if the peak response of the secondary spring during the duration of the excitation exceeds the threshold, and the corresponding LSF reads:

$$g(\mathbf{x}) = F_s - 3k_s \sqrt{\frac{\pi S_0}{4\zeta_s \omega_s^3} \left[\frac{\zeta_a \zeta_s}{\zeta_p \zeta_s (4\zeta_a^2 + \theta^2) + \gamma \zeta_a^2} \frac{(\zeta_p \omega_p^3 + \zeta_s \omega_s^3) \omega_p}{4\zeta_a \omega_a^4} \right]} \quad (45)$$

where $\omega_p = \sqrt{k_p/m_p}$, $\omega_s = \sqrt{k_s/m_s}$, $\omega_a = (\omega_p + \omega_s)/2$, $\zeta_a = (\zeta_p + \zeta_s)/2$, $\gamma = m_s/m_p$ and $\theta = (\omega_p - \omega_s)/\omega_a$. All the uncertain parameters are lognormally distributed random variables and their distribution parameters are listed in Table 4. We transform the LSF in Eq. (45) into standard normal space via an isoprobabilistic transformation. A reference value of the failure probability is obtained by MCS with 10^8 samples as $P_f = 4.42 \times 10^{-5}$.

Table 4: Random variables and their distribution parameters in Example 4.3

Variable	m_p	m_s	k_p	k_s	ζ_p	ζ_s	F_s	S_0
Mean	1.5	0.01	1	0.01	0.05	0.02	22	100
Cov	0.1	0.1	0.2	0.2	0.4	0.5	0.1	0.1

The results are listed in Table 5. They show that both the enhanced SDIS and SuS provide the desired results, but the enhanced SDIS outperforms the SuS in this example. For this challenging problem, the standard SDIS provides a severely biased estimate since there are multiple roots in several important directions, as shown in Figs. 2 and 3.

Table 5: Reliability analysis results for example 4.1 (Reference value: $P_f = 4.42 \times 10^{-5}$)

Method	$\mathbb{E}(\hat{P}_f)$	$\mathbb{E}(\delta_{\hat{P}_f})$	$\delta(\hat{P}_f)$	$\mathbb{E}(N_t)$	relEff
SuS	4.54×10^{-5}	0.31	0.45	5145	20.89
Enhanced SDIS	4.16×10^{-5}	0.21	0.40	5698	27.92
Standard SDIS	1.27×10^{-5}	0.19	0.30	13412	3.28

4.4. High dimensional series system problem with two nonlinear branches

In this section, we test the performance of the enhanced SDIS method by a nonlinear series system. The LSF is given by:

$$G(\mathbf{u}) = \min \left\{ \beta - \frac{1}{\sqrt{n}} \sum_{i=1}^n u_i + (u_1 - u_2)^2/10, \beta + \frac{1}{\sqrt{n}} \sum_{i=1}^n u_i + (u_1 - u_2)^2/10 \right\} \quad (46)$$

In this example, we set $\beta = 3.5$, and the reference failure probability is 2.92×10^{-4} , which is independent of the number of input variables n . To better understand the shape the LSF considered here, Fig. 8 visualizes the limit state surface for $n = 2$. One can see that there are two failure domains in opposite sides of the origin.

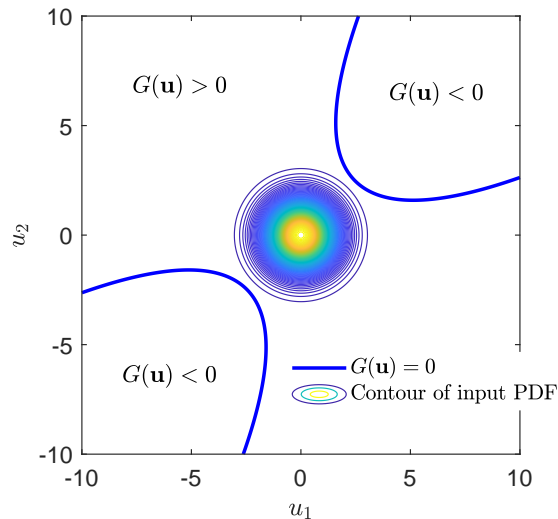


Figure 8: Two dimensional visualized LSF of example 4.4.

We test the performance of the enhanced SDIS for varying input dimen-

sions n . The results for all methods are reported in Table 6. All methods give reasonable accuracy and efficiency in all settings. The enhanced SDIS outperforms SuS for $n = 10$. However, the performance of the enhanced SDIS degenerates with the rise of input dimension, and SuS is superior for $n = 100$ and $n = 1000$. Overall, the enhanced SDIS is comparable to SuS in this problem and it always outperforms the standard SDIS.

Table 6: Reliability analysis results for example 4.4

$n = 10$	$\mathbb{E}(\hat{P}_f)$	$\mathbb{E}(\hat{\delta}_{\hat{P}_f})$	$\delta_{\hat{P}_f}$	$\mathbb{E}(N_t)$	relEff
SuS	2.95×10^{-4}	0.25	0.28	4404	9.68
Enhanced SDIS	2.93×10^{-4}	0.17	0.26	2922	17.39
Standard SDIS	2.94×10^{-4}	0.19	0.25	3936	13.81
$n = 100$	$\mathbb{E}(\hat{P}_f)$	$\mathbb{E}(\hat{\delta}_{\hat{P}_f})$	$\delta_{\hat{P}_f}$	$\mathbb{E}(N_t)$	relEff
SuS	2.94×10^{-4}	0.25	0.29	4405	9.24
Enhanced SDIS	2.84×10^{-4}	0.24	0.31	4531	8.15
Standard SDIS	2.88×10^{-4}	0.25	0.29	6829	6.11
$n = 1000$	$\mathbb{E}(\hat{P}_f)$	$\mathbb{E}(\hat{\delta}_{\hat{P}_f})$	$\delta_{\hat{P}_f}$	$\mathbb{E}(N_t)$	relEff
SuS	3.03×10^{-4}	0.25	0.29	4397	8.69
Enhanced SDIS	2.87×10^{-4}	0.27	0.31	5260	7.06
Standard SDIS	2.73×10^{-4}	0.28	0.29	8946	5.01

4.5. High dimensional nonlinear example

We now test the performance of the enhanced SDIS method with the following LSF in standard normal input space [19]:

$$G(\mathbf{u}) = C_a + \sum_{i=1}^n \ln(\Phi^{-1}(-u_i)). \quad (47)$$

The function in Eq. (47) is highly nonlinear. The reference value of probability of failure is $P_f = 1 - F_Y(C_a)$, where Y is a Gamma distributed random variable with shape parameter n and scale parameter $\lambda = 1$. In this example, we vary the input dimension from $n = 10$ to 1000. We adjust the value of C_a to fix $P_f = 5 \times 10^{-5}$ for different n . The visualized limit state

surface for $n = 2$ is depicted in Fig. 9. One can see that the 2-dimensional limit state surface is nonlinear and it has a convex safe domain.

The results are summarized in Table 7. Enhanced SDIS yields good results for various input dimensions n . It outperforms SuS for $n = 10$. With increasing input dimension, the performance of the enhanced SDIS degenerates gradually, and it is inferior to SuS for $n = 100$ and $n = 1000$. In addition, it is observed that the enhanced SDIS always outperforms the standard SDIS considerably, which is due to the increased efficiency of the proposed Kriging-based root-finding algorithm compared to the one applied in standard SDIS.

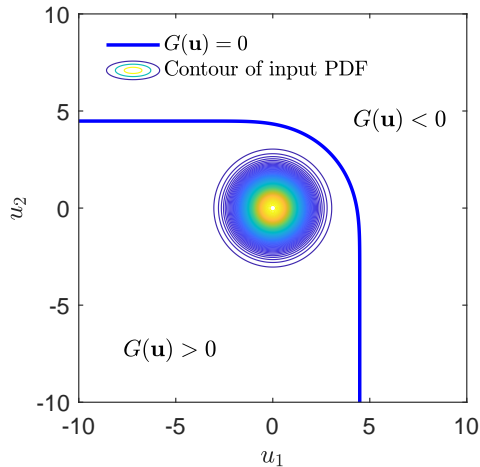


Figure 9: Two dimensional visualized LSF of example 4.5.

5. Conclusion

We presented an enhanced sequential directional importance sampling (SDIS) method for structural reliability analysis. The main contributions that lead to improved performance are twofold. First, we proposed to estimate the first integral in SDIS with Subset Simulation (SuS) in problems with narrow failure domains. Second, we developed a Kriging-based active learning algorithm that is able to identify multiple roots within a specified search interval and has increased efficiency compared to the root-finding algorithm used in the standard SDIS.

Table 7: Reliability analysis results for example 4.5

$n = 10$	$\mathbb{E}(\hat{P}_f)$	$\mathbb{E}(\hat{\delta}_{\hat{P}_f})$	$\delta_{\hat{P}_f}$	$\mathbb{E}(N_t)$	relEff
SuS	5.04×10^{-5}	0.27	0.32	5094	38.40
Enhanced SDIS	4.81×10^{-5}	0.16	0.24	2070	170.76
Standard SDIS	4.99×10^{-5}	0.17	0.25	3254	102.25
$n = 100$	$\mathbb{E}(\hat{P}_f)$	$\mathbb{E}(\hat{\delta}_{\hat{P}_f})$	$\delta_{\hat{P}_f}$	$\mathbb{E}(N_t)$	relEff
SuS	4.94×10^{-5}	0.27	0.326	5105	37.54
Enhanced SDIS	4.76×10^{-5}	0.22	0.44	4211	26.53
Standard SDIS	4.88×10^{-5}	0.22	0.45	6905	15.18
$n = 1000$	$\mathbb{E}(\hat{P}_f)$	$\mathbb{E}(\hat{\delta}_{\hat{P}_f})$	$\delta_{\hat{P}_f}$	$\mathbb{E}(N_t)$	relEff
SuS	5.13×10^{-5}	0.28	0.339	5089	32.39
Enhanced SDIS	4.91×10^{-5}	0.25	0.51	4988	16.09
Standard SDIS	4.70×10^{-5}	0.25	0.50	11851	7.48

Several benchmarks were investigated to compare the performance of the enhanced SDIS to that of standard SDIS and SuS. The results demonstrated that the enhanced SDIS outperforms the standard one in terms of efficiency and robustness. It is a versatile reliability analysis method, which can potentially address various challenging reliability analysis problems, i.e., problems with highly nonlinear limit state function, low magnitude of failure probability, multiple disjoint failure domains and high-dimensional input parameter. As with standard SDIS, the performance of the enhanced SDIS still degenerates with increasing input variable dimension. This is attributed to the fact that the variance of the conditional failure probability $\Pr(G(\sigma R \mathbf{a}) \leq 0)$ rises gradually when the input dimension increases, thus requiring more intermediate steps to achieve convergence in SDIS. In problems with more than 100 input variables, SuS still outperforms the enhanced SDIS.

Appendix A. The ordinary Kriging model

In the ordinary Kriging model, the one-dimensional computational model $y = G(\sigma r \mathbf{a})$ in direction \mathbf{a} is assumed to be a Gaussian process

$$Y(r) = \beta_0 + Z(r),$$

where $\beta_0 \in \mathbb{R}^m$ is the mean of $Y(r)$, and $Z(r)$ is a stationary Gaussian process with zero mean and covariance function given by

$$\text{Cov}(Z(r), Z(\hat{r})) = \sigma_0^2 k(r, \hat{r}; \theta),$$

where σ_0^2 is the variance of $Z(r)$, and $k(r, \hat{r}; \theta)$ represents the spatial correlation between r and \hat{r} with the correlation length controlled by the hyper-parameter θ .

Under the Gaussian process assumption, the joint distribution of $Y(r)$ and $\mathbf{Y} = [Y(r^{(1)}), \dots, Y(r^{(M)})]^\text{T}$ at the sampled locations is multivariate Gaussian, namely

$$\begin{bmatrix} Y(r) \\ \mathbf{Y} \end{bmatrix} \sim \mathcal{N} \left(\begin{bmatrix} \beta_0 \\ \beta_0 \mathbf{F} \end{bmatrix}, \sigma_0^2 \begin{bmatrix} 1 & \mathbf{k}^\text{T}(r) \\ \mathbf{k}(r) & \mathbf{K} \end{bmatrix} \right),$$

where $\mathbf{F} := [1, \dots, 1]^\text{T} \in \mathbb{R}^M$ and

$$\begin{aligned} \mathbf{K} &:= k(r^{(i)}, r^{(j)}; \theta), i, j = 1, \dots, M, \\ \mathbf{k}(r) &:= k(r^{(i)}, r; \theta), i = 1, \dots, M. \end{aligned}$$

Given the observation values $\mathbf{Y} = [G(\sigma_i r^{(1)} \mathbf{a}), \dots, G(\sigma_i r^{(M)} \mathbf{a})]^\text{T}$, the predictive distribution of $Y(r)$ is given by

$$\hat{Y}(r) \sim \mathcal{N}(\mu(r), s^2(r)),$$

where the mean and variance are given by

$$\begin{aligned} \mu(r) &= \beta_0 + \mathbf{k}^\text{T}(r) \mathbf{K}^{-1} (\mathbf{Y} - \beta_0 \mathbf{F}), \\ s^2(r) &= \sigma_0^2 (1 - \mathbf{k}^\text{T}(r) \mathbf{K}^{-1} \mathbf{k}(r) + \mathbf{u}^\text{T}(r) (\mathbf{F}^\text{T} \mathbf{R}^{-1} \mathbf{F})^{-1} \mathbf{u}(r)). \end{aligned}$$

in which $\mathbf{u}(r) = \mathbf{F}^\text{T} \mathbf{K}^{-1} \mathbf{k}(r) - 1$.

In ordinary Kriging model, the mean β_0 and variance σ_0^2 are given by

$$\begin{aligned} \beta_0 &= (\mathbf{F}^\text{T} \mathbf{K}^{-1} \mathbf{F})^{-1} \mathbf{F}^\text{T} \mathbf{K}^{-1} \mathbf{Y}, \\ \sigma_0^2 &= \frac{1}{M} (\mathbf{Y} - \beta_0 \mathbf{F})^\text{T} \mathbf{K}^{-1} (\mathbf{Y} - \beta_0 \mathbf{F}). \end{aligned}$$

The hyper-parameter θ is determined with maximum likelihood estimation method, which is equivalent to minimizing the following objective func-

tion:

$$\ell(\theta) = M \ln \sigma_0^2 + \ln [\det \mathbf{K}].$$

Appendix B. Acknowledgements

This work was supported by the Alexander von Humboldt Foundation.

References

- [1] Siu-Kui Au and James L Beck. A new adaptive importance sampling scheme for reliability calculations. *Structural safety*, 21(2):135–158, 1999.
- [2] Siu-Kui Au and James L Beck. Estimation of small failure probabilities in high dimensions by subset simulation. *Probabilistic engineering mechanics*, 16(4):263–277, 2001.
- [3] Siu-Kui Au and JL Beck. Important sampling in high dimensions. *Structural safety*, 25(2):139–163, 2003.
- [4] Peter Bjerager. Probability integration by directional simulation. *Journal of Engineering Mechanics*, 114(8):1285–1302, 1988.
- [5] J-M Bourinet. Rare-event probability estimation with adaptive support vector regression surrogates. *Reliability Engineering & System Safety*, 150:210–221, 2016.
- [6] Karl Breitung. Asymptotic approximations for multinormal integrals. *Journal of Engineering Mechanics*, 110(3):357–366, 1984.
- [7] Karl Breitung. The geometry of limit state function graphs and subset simulation: Counterexamples. *Reliability Engineering & System Safety*, 182:98–106, 2019.
- [8] Frédéric Cérou, Pierre Del Moral, Teddy Furon, and Arnaud Guyader. Sequential monte carlo for rare event estimation. *Statistics and computing*, 22(3):795–808, 2012.
- [9] Jianpeng Chan, Iason Papaioannou, and Daniel Straub. Bayesian improved cross entropy method for network reliability assessment. *Structural Safety*, 103:102344, 2023.

- [10] Kai Cheng and Zhenzhou Lu. Adaptive bayesian support vector regression model for structural reliability analysis. *Reliability Engineering & System Safety*, 206:107286, 2021.
- [11] Kai Cheng, Zhenzhou Lu, Sinan Xiao, and Jingyu Lei. Estimation of small failure probability using generalized subset simulation. *Mechanical Systems and Signal Processing*, 163:108114, 2022.
- [12] Kai Cheng, Iason Papaioannou, Zhenzhou Lu, Xiaobo Zhang, and Yanping Wang. Rare event estimation with sequential directional importance sampling. *Structural Safety*, 100:102291, 2023.
- [13] Chao Dang, Marcos A Valdebenito, Matthias GR Faes, Pengfei Wei, and Michael Beer. Structural reliability analysis: A bayesian perspective. *Structural Safety*, 99:102259, 2022.
- [14] Armen Der Kiureghian. *Structural and system reliability*. Cambridge University Press, 2022.
- [15] Armen Der Kiureghian, Hong-Zong Lin, and Shyh-Jiann Hwang. Second-order reliability approximations. *Journal of Engineering mechanics*, 113(8):1208–1225, 1987.
- [16] Ove Ditlevsen, Robert E Melchers, and H Gluwer. General multi-dimensional probability integration by directional simulation. *Computers & Structures*, 36(2):355–368, 1990.
- [17] Benjamin Echard, Nicolas Gayton, and Maurice Lemaire. AK-MCS: an active learning reliability method combining Kriging and Monte Carlo simulation. *Structural Safety*, 33(2):145–154, 2011.
- [18] DJ Finney. On a method of estimating frequencies. *Biometrika*, 36(1-2):233–234, 1949.
- [19] M. Fujita and Ruediger Rackwitz. Updating first- and second-order reliability estimates by importance sampling. *Structural Engineering / Earthquake Engineering*, 5:53–59, 1988.
- [20] Sebastian Geyer, Iason Papaioannou, and Daniel Straub. Cross entropy-based importance sampling using gaussian densities revisited. *Structural Safety*, 76:15–27, 2019.

- [21] Frank Grooteman. An adaptive directional importance sampling method for structural reliability. *Probabilistic Engineering Mechanics*, 26(2):134–141, 2011.
- [22] JBS Haldane. On a method of estimating frequencies. *Biometrika*, 33(3):222–225, 1945.
- [23] Abraham M Hasofer. An exact and invariant first order reliability format. *J. Eng. Mech. Div., Proc. ASCE*, 100(1):111–121, 1974.
- [24] Jun He, Shengbin Gao, and Jinghai Gong. A sparse grid stochastic collocation method for structural reliability analysis. *Structural Safety*, 51:29–34, 2014.
- [25] Michael Hohenbichler and Rüdiger Rackwitz. Non-normal dependent vectors in structural safety. *Journal of the Engineering Mechanics Division*, 107(6):1227–1238, 1981.
- [26] Michael Hohenbichler and Ruediger Rackwitz. First-order concepts in system reliability. *Structural safety*, 1(3):177–188, 1982.
- [27] Shi-Ya Huang, Shao-He Zhang, and Lei-Lei Liu. A new active learning kriging metamodel for structural system reliability analysis with multiple failure modes. *Reliability Engineering & System Safety*, 228:108761, 2022.
- [28] Norman L Johnson, Samuel Kotz, and Narayanaswamy Balakrishnan. *Continuous Univariate Distributions*. John Wiley & Sons, 2nd edition, 1994.
- [29] Armen Der Kiureghian and Mario De Stefano. Efficient algorithm for second-order reliability analysis. *Journal of engineering mechanics*, 117(12):2904–2923, 1991.
- [30] Jack PC Kleijnen. Kriging metamodeling in simulation: A review. *European journal of operational research*, 192(3):707–716, 2009.
- [31] Nolan Kurtz and Junho Song. Cross-entropy-based adaptive importance sampling using gaussian mixture. *Structural Safety*, 42:35–44, 2013.
- [32] Pierre L’Ecuyer. Efficiency improvement and variance reduction. In *Proceedings of Winter Simulation Conference*, pages 122–132. IEEE, 1994.

- [33] Maliki Moustapha, Stefano Marelli, and Bruno Sudret. Active learning for structural reliability: Survey, general framework and benchmark. *Structural Safety*, 96:102174, 2022.
- [34] Iason Papaioannou, Wolfgang Betz, Kilian Zwirgmaier, and Daniel Straub. Mcmc algorithms for subset simulation. *Probabilistic Engineering Mechanics*, 41:89–103, 2015.
- [35] Iason Papaioannou, Sebastian Geyer, and Daniel Straub. Improved cross entropy-based importance sampling with a flexible mixture model. *Reliability Engineering & System Safety*, 191:106564, 2019.
- [36] Iason Papaioannou, Costas Papadimitriou, and Daniel Straub. Sequential importance sampling for structural reliability analysis. *Structural safety*, 62:66–75, 2016.
- [37] Iason Papaioannou and Daniel Straub. Combination line sampling for structural reliability analysis. *Structural Safety*, 88:102025, 2021.
- [38] HJ Pradlwarter, Gerhart Iwo Schueller, Phaedon-Stelios Koutsourelakis, and Dimos C Charmpis. Application of line sampling simulation method to reliability benchmark problems. *Structural safety*, 29(3):208–221, 2007.
- [39] Mohsen Rashki. SESC: A new subset simulation method for rare-events estimation. *Mechanical Systems and Signal Processing*, 150:107139, 2021.
- [40] Mohsen Ali Shayanfar, Mohammad Ali Barkhordari, Moien Barkhori, and Mohammad Barkhori. An adaptive directional importance sampling method for structural reliability analysis. *Structural Safety*, 70:14–20, 2018.
- [41] Rui Teixeira, Maria Nogal, and Alan O’Connor. Adaptive approaches in metamodel-based reliability analysis: A review. *Structural Safety*, 89:102019, 2021.
- [42] Ziqi Wang, Marco Broccardo, and Junho Song. Hamiltonian monte carlo methods for subset simulation in reliability analysis. *Structural Safety*, 76:51–67, 2019.

- [43] Ziqi Wang and Junho Song. Cross-entropy-based adaptive importance sampling using von mises-fisher mixture for high dimensional reliability analysis. *Structural Safety*, 59:42–52, 2016.
- [44] Pengfei Wei, Yu Zheng, Jiangfeng Fu, Yuannan Xu, and Weikai Gao. An expected integrated error reduction function for accelerating bayesian active learning of failure probability. *Reliability Engineering & System Safety*, 231:108971, 2023.
- [45] Jianhua Xian and Ziqi Wang. Relaxation-based importance sampling for structural reliability analysis. *Structural Safety*, 106:102393, 2024.
- [46] Jun Xu and Chao Dang. A new bivariate dimension reduction method for efficient structural reliability analysis. *Mechanical Systems and Signal Processing*, 115:281–300, 2019.
- [47] Xufeng Yang, Yongshou Liu, Yi Gao, Yishang Zhang, and Zongzhan Gao. An active learning kriging model for hybrid reliability analysis with both random and interval variables. *Structural and Multidisciplinary Optimization*, 51:1003–1016, 2015.
- [48] Xiaobo Zhang, Zhenzhou Lu, and Kai Cheng. Cross-entropy-based directional importance sampling with von mises-fisher mixture model for reliability analysis. *Reliability Engineering & System Safety*, 220:108306, 2022.
- [49] Yan-Gang Zhao and Tetsuro Ono. Moment methods for structural reliability. *Structural safety*, 23(1):47–75, 2001.